JOURNAL OF MATERIALS SCIENCE 28 (1993) 2449–2454

Organometallic route to dimolybdenum carbide via a low-temperature pyrolysis of a dimolybdenum alkyne complex

J.-M. GIRAUDON, L. LECLERCQ, G. LECLERCQ
Laboratoire de Catalyse Hétérogène et Homogène, UA CNRS no. 402, Université des Sciences et Techniques de Lille Flandres-Artois, 59655 Villeneuve d'Ascq Cédex, France

A. LOFBERG, A. FRENNET
Unité de Recherche sur la Catalyse, Université Libre de Bruxelles, CP243, B-1050 Bruxelles, Belgium

Pyrolytic transformation of the complex $Cp_2Mo_2(CO)_4(dmad)$ (Cp = cyclopentadienyl, dmad = dimethylacetylenedicarboxylate) under hydrogen at 550 °C gives, after a passivation step, Mo_2C with an excess of carbon and oxygen. These impurities can be withdrawn with an appropriate reductive post-treatment. Based on thermogravimetric analyses and pyrolysis mass spectroscopy performed on the precursor, a preliminary decomposition scheme has been proposed.

1. Introduction

Growing attention is focused on advanced ceramic materials such as carbides because of possible multiple applications due to their intrinsic properties such as hardness, corrosion resistance and thermal stabilities. One potential way to prepare these materials consists of the pyrolysis of designed organometallic precursors. Thus, faced with the common industrial processes for the production of transition metal carbides, which are expensive in terms of equipment and energy due to the lengthy time and high temperatures of carburization, organometallic chemistry appears to be a new and flexible method for obtaining these materials. General design criteria for the synthesis of material precursors have been set out by Laine and Hirschon [1]. The premetallics must be non-volatile, tractable compounds containing multiple metal carbon bonds to enhance the formation of metal carbides upon pyrolysis. Based on X-ray and Auger spectroscopy studies, Laine and Hirschon have shown that the alkyne complex $Cp_2W_2(CO)_4(dmad)$, where Cp = cyclopentadienyl and dmad = dimethylacetylenedicarboxylate, can lead to W_2C at 750 °C by pyrolysis under appropriate conditions [2]. In accordance with these results, we report here the pyrolysis under hydrogen of the molybdenum complex $Cp_2Mo_2(CO)_4(dmad)$ at 550 °C to give Mo_2C.

2. Experimental procedure

2.1. Synthesis

The preparation of the organometallic complex was carried out under a dry and oxygen-free nitrogen atmosphere using Schlenk tubes. Solvents were distilled by standard techniques and thoroughly deoxygenated before use.

$Mo(CO)_6$ and $H_3CO_2C{-}C{\equiv}C{-}CO_2CH_3$ were purchased from Aldrich and used without further purification. $\{CpMo(CO)_2\}_2$ was synthesized by the usual route given in the literature [3].

2.1.1. $Cp_2Mo_2(CO)_4(dmad)$

This was prepared as previously described by Bailey *et al.* [4]. To a stirred solution of $\{CpMo(CO)_2\}_2$ (0.3 g = 6.90 mmol) in toluene, 2 ml, 16 mmol dimethylacetylenedicarboxylate was added at room temperature via a syringe. After 6 h reaction, the solvent was removed by vacuum and the residue was pumped overnight to remove excess alkyne. Red needles were obtained after recrystallization (yield = 40%).

Data for the molybdenum complex are as follows:

Anal. calc. for $Mo_2C_{20}H_{16}O_8$: C 41.69; H 2.80; Mo 33.3.
Found: C 42.4; H 2.83; Mo 33.2
Infrared (KBr, cm^{-1}) 2005 w, 1975 s, 1965 m, 1940 s, 1920 s, 1860 m, 1680 s.

2.1.2. Mo_2C

The pyrolysis was performed by placing the red crystals of $Cp_2Mo_2(CO)_4$ (dmad) in a stainless steel boat. This was introduced into a quartz flow reactor which fitted into a vertical furnace. The temperature was regulated at 1 °C in a range of 15 cm. Prior to the heat treatment, the sample was flushed with nitrogen for 30 min (flow rate 3 l h^{-1}). After the passage of hydro-

0022–2461

gen (flow rate 6 l h^{-1}) through the apparatus {100 °C h^{-1} (550 °C, 2 h)}, the sample was allowed to cool to room temperature. After 30 min purging with nitrogen, the powder was submitted to a passivation step at room temperature under a flowing mixture of 1% oxygen in nitrogen.

Nitrogen U, hydrogen U and air B were provided by Air Liquide. The hydrogen was further purified by interposing successively a palladium diffusion process, silica gel and molecular sieve 13 X between the cylinder and the quartz inlet tube.

2.2. Physical measurements

Elemental analyses were performed by the Service Central de Microanalyse du CNRS, Vernaison, France. Infrared spectra were run using a Perkin–Elmer 1430 spectrophotometer and KBr pellets.

X-ray diffraction (XRD) patterns of the samples were obtained using a Philips PW1008 apparatus (CuK_α radiation = 0.154 178 nm, nickel filter). X-ray photoelectron spectroscopy (XPS) measurements were carried out with an AEI ES 200B spectrophotometer equipped with an aluminium anode ($h\nu$ = 1486.6 eV, 300 W). C1s arising from *in situ* contamination (BE = 285 ± 0.2 eV) [5] was used as reference for the calculation of binding energies (BE).

The thermogravimetric analyses (TGA) were performed with a Sartorius vacuum microbalance instrument in a hydrogen-flowing atmosphere (flow rate 3 l h^{-1}). The heating rate was 100 °C h^{-1} and the sample weights in the range 9–10 mg.

The pyrolysis–mass spectroscopy analyses were performed using a Balzers QMG 420-3 quadrupole mass spectrometer. Data collection and control of the instrument were conducted by an IBM compatible computer equipped with the Quadstar 420 v3.03 (Balzers) software. The temperature was automatically regulated by means of a control unit (Eurotherm type 818) coupled with a chromel–alumel thermocouple junction. Measurement of the temperature was given by a Eurotherm type 842 indicator. The gases used were argon (UCAR purity 5.0), hydrogen (UCAR purity "certified standard" 9.93% hydrogen in argon), oxygen (BOC purity "Alpha Standard", 10% oxygen in argon). The passivated sample (20 mg) of Mo_2C was placed in a mixed quartz reactor. After purging with argon until the total disappearance of the mass signal peaked at m = 32 assigned to oxygen, the pyrolysis was conducted in a flowing hydrogen–argon mixture (10/90, flow rate 6 cm^3 min^{-1}) at atmospheric pressure up to 800 °C (6 °C min^{-1}).

The pyroprobe was interfaced to the mass spectrometer via a stainless steel line using a jet separator to remove most of the carrier gas. The ionization was accomplished by electron impact at an energy of 70 eV. After passivation (room temperature, oxygen 2% in argon, 30 min) the sample was then submitted to a hydrogen treatment (hydrogen 10% in argon, rate 6 cm^3 min^{-1}). In each case, the gaseous products formed were continuously analysed by mass spectroscopy.

The pyrolysis of the organometallic complex consisted first in the determination of the principal mass peaks, here in the range 0–100, implicated in the decomposition process. On purpose, 10.1 mg of the precursor were flushed with hydrogen (10% hydrogen in argon, rate 6 cm^3 min^{-1}) to 550 °C (10 °C min^{-1}). The mass spectra were obtained in the scan analogue mode. The total time for a run was 30 s. Secondly, the experiment was repeated with a lower temperature ramp (3 °C min^{-1}) which allowed us to record the selected masses, i.e. 2–12–15–18–28–31–32–40–41–42–43–55–66–91 versus time and temperature. This gave details regarding the temperature profiles at which the various pyrolysates were released.

3. Results

In order to work well below the usual temperatures needed to form Mo_2C in the metallurgical industry which are higher than 1200 °C, a programmed thermoreduction of dmad was carried out using the gravimetric method. As shown in Fig. 1, the differential curve exhibits five peaks above 100 °C corresponding to the successive removals of the different ligands linked to the molybdenum atoms. At 476 °C, the decomposition is complete. By considering the global weight loss, e.g. neglecting the weight loss before 50 °C probably due to the elimination of solvents of recrystallization, we found the formula Mo_2C (within a margin of error of ± 2%). Owing to these results, samples of dmad were pyrolysed at 550 °C in flowing hydrogen for 2 h. After a passivation step (1% oxygen in nitrogen) a grey powder of Mo_2C was obtained. Based on the metal, the yield of the reaction is ~ 90%.

The infrared spectrum of the sample after reaction under hydrogen and passivation (Fig. 2) exhibits none of the carbonyl valence vibration bands characteristic of the precursor. Noteworthy are very small peaks at 2140 and 2155 cm^{-1} which can tentatively be assigned to some strong carbonyl valence vibration bands.

The XRD pattern is rather ill-defined and suggests the formation of amorphous or microcrystalline products. It must be pointed out that the reductive treatments are not without effect upon the bulk of the material. X-ray studies carried out on samples submitted to a hydrogen flow (3 l h^{-1}) at different temperatures (600, 800, 900 °C) for 15 h showed that the

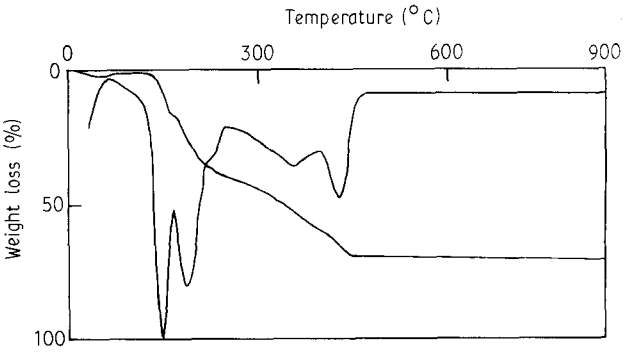

Figure 1 TGA profile of the organometallic precursor (H_2 = 3 l h^{-1}, T = 100 °C h^{-1}).

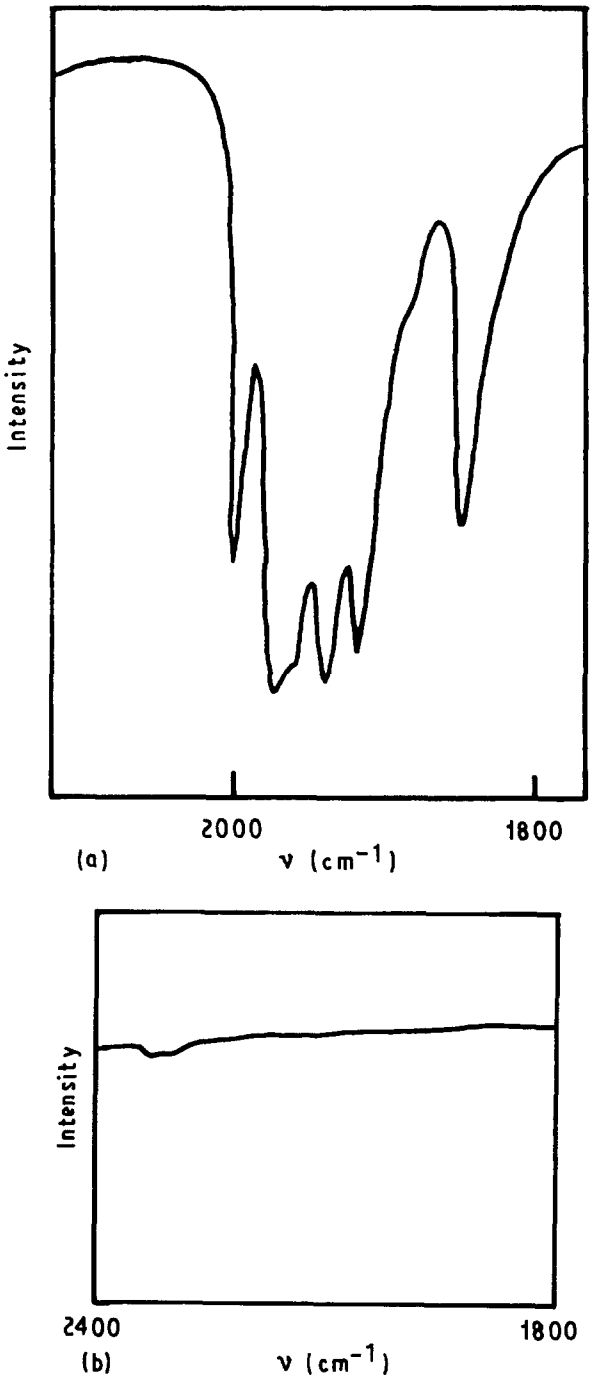

Figure 2 Evolution of the carbonyl bands in infrared spectroscopy. (a) Infrared spectrum of the organometallic precursor $Cp_2Mo_2(CO)_4$(dmad). (b) Infrared spectrum of the molybdenum carbide after synthesis.

different bands become progressively refined and well resolved after passivation, indicating an increase in the size of the crystallites as temperature rises. Direct comparison with the XRD pattern of a reference sample of Mo_2C with a low surface area proves the formation of a rather pure bulk hexagonal close packed Mo_2C at 800 °C (cf. Table I). The presence of molybdenum metal after a treatment in hydrogen at 900 °C should be noted in addition to the detection of molybdenum carbide.

The surface composition of the samples was analysed by X-ray photoelectron spectroscopy (XPS). The C1s signal (Fig. 3a) centred around 285 eV appears to be rather large with a half signal width of 2.62 eV, which is much higher than the usual value of 1.6 eV [6]. This signal is asymmetrical, indicating the presence of different carbons. The main peak centred at 285 eV is ascribed to the presence of a substantial amount of polluting carbon or "free carbon". The peak at a lower binding energy is characteristic of the presence of carbidic carbon at about 283.4 eV, and the shoulders at higher BE are mainly due to oxidized carbon contamination.

XPS results indicate that the $Mo3d_{5/2}$ (Fig. 4) peaks at 228.7 eV, which agrees with a Mo_2C phase [7], the carbidic contribution being around 50% as indicated by Equation 1. Quantitative determination of the average composition of the layer analysed by XPS was carried out using the formula proposed by Ward *et al.* [8]

$$n_X/n_Y = I_X/I_Y(\sigma_Y/\sigma_X)(E_Y/E_X)^{1.7} \quad (1)$$

where n_X/n_Y is the atomic ratio between the elements X and Y, I_X and I_Y are the photopeak areas, σ_X and σ_Y are the cross-sections, E is the kinetic energy corresponding to the level under consideration. Quantification of the carbon species is obtained by deconvoluting the C1s spectra using peak parameters measured by separately analysing the C1s spectra of Mo_2C and polluting carbon on rather pure samples. Subtraction of these two components from the total C1s XPS area allowed us to determine the oxidized carbon, C_{ox}, contribution. The absolute error inherent in such determinations can be considerable, although the relative error among all the samples is expected to be low, provided all decompositions are made with constant parameters. The results are reported in Table II. They show the contamination of the samples with free carbon and oxygen which arises during the passivation step and/or the decomposition process.

Although the O1s line centred at 533.2 eV is rather symmetrical (half peak width = 3.1 eV), its origin is not clear. The high O1s energies indicate very low electron densities on the oxygen atoms. Such values have been reported in the literature for O1s BE in poly(methyl methacrylate) at 532.4 and 534 eV [6] and can suggest the formation of similar polymers inside the XPS layer. The chemical analysis (Mo 90.41, C 8.14, O 1.44) gives an empirical formula $Mo_2C_{1.4}O_{0.2}$ and confirms the existence of Mo_2C together with an excess of carbon and oxygen. Based on the values of the XPS and chemical formula we conclude that the carbon and oxygen are mainly at the surface of the carbide.

In order to obtain a surface as clean as possible, post-treatments under hydrogen were performed at different temperatures and followed by XPS studies. The successive reductions were carried out in a reactor attached to the spectrophotometer via a dry-nitrogen-purged glove box. Figs 3 and 4 show the evolution of the C1s and of the Mo3d spectra of Mo_2C after the passivation treatment, and after successive reductions in hydrogen for 15 h at 250 °C, for 4 h at 500 °C and for 4 h at 600 °C. The efficiency of the cleaning was quantified by considering the modifications of the XPS surface areas (Table II). It clearly shows that oxygen is progressively removed from the surface

TABLE I X-ray data for Mo_2C carbide

2θ (deg)	d_{exp} (nm)	I/I_0	d_{th} (nm)	I/I_0	hkl
34.5	2.5974	m	2.60	20	100
38.0	2.3658	m	2.37	30	002
39.5	2.2794	S	2.28	100	101
52.12	1.7530	m	1.750	16	102
61.5	1.5064	m	1.503	12	110
69.5	1.3513	m	1.349	18	103

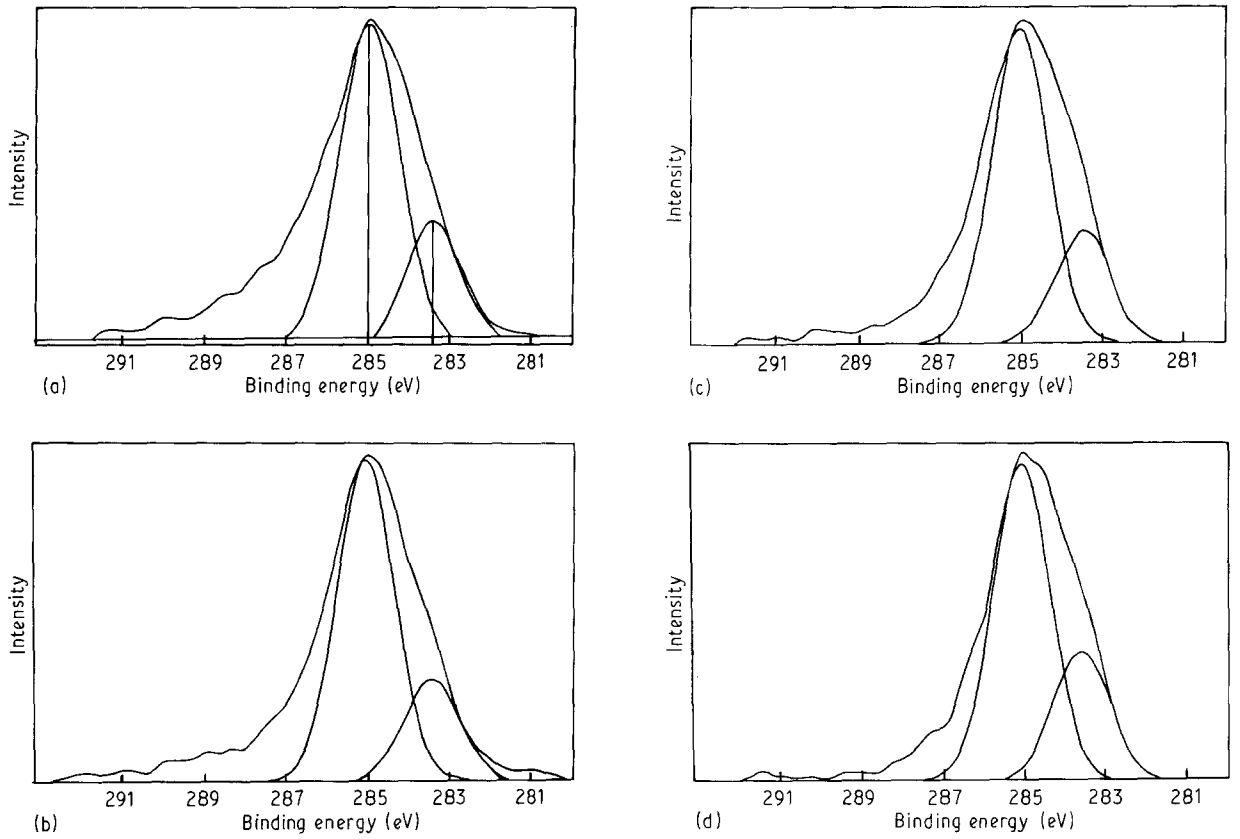

Figure 3 C1s XPS spectra of the molybdenum carbide: (a) RT after passivation; (b) after hydrogen post-treatment (HPT) 250 °C, 15 h; (c) HPT 500 °C, 4 h; (d) HPT 600 °C, 4 h.

because the O/Mo atomic ratio decreased from 3.2 to 2.6 between room temperature and 600 °C. At 500 °C, after hydrogen post-treatment (HPT), the Mo3d spectrum showed a well-resolved doublet spaced 3.1 eV apart which characterizes a molybdenum free of oxides. On the other hand, carbon removal began to be detected at higher temperature (500 °C), the C_{ox} component being more easily removed than the free carbon. Unexpectedly, no further improvement was noticeable at a temperature of 600 °C. This could reduce the obtention at this temperature of a reactive surface which could react more easily with adventitious contaminants in the glove box during the transfer of the sample to the XPS apparatus.

Additional information is provided by slow pyrolysis–mass spectroscopy (PMS). Fig. 5 shows the temperature-programmed pyrolysis–mass curves under hydrogen of the molybdenum carbide Mo_2C, obtained after the passivation step. The relative ion current versus temperature diagrams include only the masses characteristic of the gases which usually evolve during such experiments i.e. CH_4, CO, CO_2 and H_2O (see Table III). Below 470 °C no reaction was observed. The formation of CO and CH_4 begins at 473 and 553 °C, respectively, and reaches a maximum at 673 and 730 °C. After 40 min at 790 °C, removal of CO and CH_4 still continues. Considering that the carbon evolves in the form of CO and CH_4, and oxygen as CO, the carbon and oxygen contents which disappear during the reaction can be estimated in terms of molecules from the equation

$$n_X = I_X d(N/f_X)RT \quad (2)$$

where n_X is the number of molecules of the gas X, I_X (A min^{-1}) is the surface area, d (cm^3 min^{-1}) the flow rate, and f_X (A $torr^{-1}$) the sensibility factor of gas X. This parameter is readily obtained by calibration against the sensibility factor of the gas vector (i.e. argon). R is the gas constant, T the temperature of the experiment (here $T = 298$ K) and N the Avogadro constant. Given the initial mass of molybdenum carbide, we obtain the formula $Mo_2C_{1.2}O_{0.07}$. This

TABLE II Surface composition of the molybdenum carbide from XPS measurements

Samples	Mo(%) carbidic	Mo(%) oxide	C_t/Mo	O/Mo	C_c/C_t	C_{ox}/C_t	C_f/C_t
A[a]	51	49	2.0	3.2	0.15	0.34	0.51
B[b]	64	36	2.0	2.9	0.16	0.30	0.54
C[c]	100	0	1.7	2.6	0.21	0.22	0.57
D[d]	100	0	1.7	2.6	0.23	0.17	0.60

[a] After the passivation step.
[b] After 4 h under H_2 at 250 °C.
[c] After 4 h under H_2 at 500 °C.
[d] Ater 4 h under H_2 at 600 °C.
C_t = total carbon, C_c = carbidic carbide, C_{ox} = oxidized carbon, C_f = free carbon, O = oxygen.

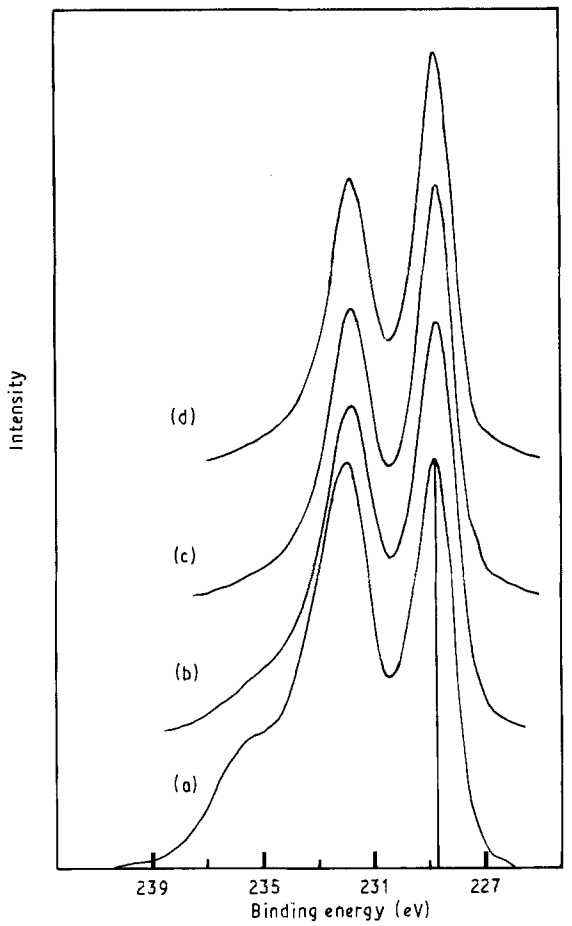

Figure 4 Mo3d spectra of the molybdenum carbide: (a) room temperature after passivation; (b) after hydrogen post-treatment (HPT) 250 °C, 15 h; (c) HPT 500 °C, 4 h; (d) HPT 600 °C, 4 h.

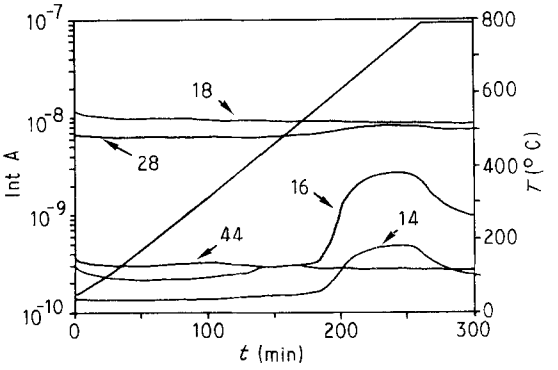

Figure 5 Slow pyrolysis–mass spectrum of the molybdenum carbide under hydrogen–argon flow (10/90) after the passivation step. The curves are labelled with the molecular weights of the species being monitored.

TABLE III Molecular weights and most probable structures of species found in the mass spectroscopy experiments

Molecular weights	Compounds
14	CH_2
16	CH_4
18	H_2O
28	CO
44	CO_2

clearly shows that at this temperature the impurities can be withdrawn to lead to a pure material over several hours at 790 °C.

The detailed mechanism of decomposition of the organometallic compound appears to be rather complex. The thermogravimetric curve exhibits five main steps which are not clearly separated. The pyrolysis–mass spectroscopy curves of dmad in the form of bulk crystals are shown in Figs 6 and 7. These relative ion currents versus temperature diagrams included only species found to be present in the highest concentrations (see Table IV). Based on the results obtained from thermogravimetric analyses and PMS, Table V indicates, for each step of decomposition, the experimental and theoretical percentages of weight loss with respect to the assumed ligand removal. Loss of solvent of recrystallization (i.e. toluene $m/z = 92$) and CO bonded to the molybdenum atoms, occurs in the first step. Further degradation appears to be the cleavage of the carbomethoxy groups of the alkyne. This is directly supported by the formation, on the one hand, of CH_3OH and CO, and on the other hand of CH_4 and CO in accordance with the two decomposition pathways

$$-CO-\overset{1}{|}-O-\overset{2}{|}-CH_3 + \tfrac{1}{2}H_2 \begin{cases} \xrightarrow{1} CO + CH_3OH \\ \xrightarrow{2} CO_2 + CH_4 \end{cases} \quad (3)$$

The third peak presumably consists of the loss of another CO. The last two steps were assumed to arise

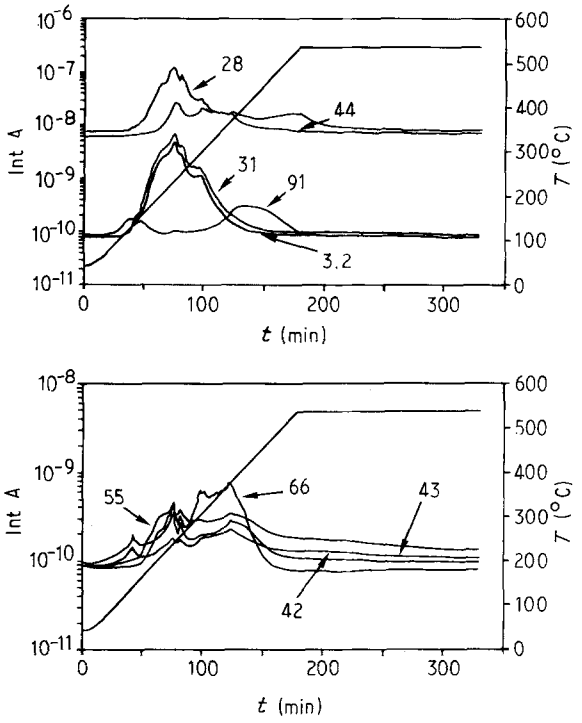

Figure 6 Slow pyrolysis–mass spectrum of $Cp_2Mo_2(CO)_4$(dmad) under hydrogen–argon flow (10/90) after the passivation step. The curves are labelled with the molecular weight of the species being monitored.

TABLE IV Molecular weights and most probable structures of species found in the mass spectroscopy experiments

Molecular weights	Compounds
15	$CH_3^{\bullet}$
28	CO
31	CH_3O
32	CH_3OH
42	CH_3–$(CH_2)_2$–$CH_2^{\bullet}$
43	CH_3–$(CH_2)_2$–CH_3
55	Organic fragments
66	C_5H_6
91	$C_7H_7^{\bullet}$

mainly from the cleavage of the two cyclopentadienyl which give little fragmentation. Contrary to expectation, the loss of CO exhibits a peak at relatively high temperatures around 530 °C. The removal of CH_4 as the last gas product of the decomposition process is notable.

TABLE V Steps of decomposition of $Cp_2Mo_2(CO)_4$(dmad)

Steps	Peak temp. (°C)	Ligands departure	Theoretical weight loss (%)	Experimental weight loss (%)
1	132	2 CO	9.72	12.1
2	196	2 CO_2CH_3	20.49	19.6
3	234	1 CO	4.86	4.7
4	377	2 C_5H_5		
		1 CO	29.54	29.9
5	453	1 C		

In conclusion, we emphasize that decomposition of the organometallic species $Cp_2Mo_2(CO)_4$(dmad) under hydrogen at low temperatures constitutes a valuable approach to molybdenum carbide Mo_2C. The main limitation of the method is the presence of hydrocarbon impurities. However, these impurities can be minimized and totally removed by a post-treatment under hydrogen, as shown by the PMS analyses. In order to develop the basic concepts of this new and promising field of organometallic research, further decompositions of new precursors are in progress.

Acknowledgements

We thank Ms Guelton for performing the thermogravimetric analysis, Mr Rémy for performing the X-ray diffraction studies, and particularly Mr L. Gengembre and Dr M. Dufour for helpful discussions.

References

1. R. LAINE and A. HIRSCHON, in "Better Ceramics Through Chemistry II", edited by C. J. Brinker and D. E. Clark (Materials Research, New York, 1984) p. 373.
2. *Idem*, NATO ASI Series, Ser. E (1988) p. 21.
3. E. FISCHER and L. PRUETT, *Inorg. Synth.* **7** (1963) 274.
4. W. BAILEY, M. CHISHOLM, F. COTTON and L. RANKEL, *J. Amer. Chem. Soc.* **98** (1976) 9744.
5. A. CHRISTIE, in "Methods of Surface Analysis. Techniques and Applications", edited by J. M. Walls (Cambridge University Press, Cambridge, 1989) p. 149.
6. C. WAGNER, W. RIGGS, L. DAVIS and J. MOULDER, in "Handbook of X-Ray Photoelectron Spectroscopy", edited by G. E. Muilenberg (1979) p. 38.
7. M. PROVOST, Doctor Engineer Thesis, University of Poitiers (1984).
8. M. WARD, M. LIN and J. LUNSFORD, *J. Catal.* **50** (1977) 306.

Received 4 March
and accepted 24 August 1992